

# Theoretical calculations of interactions between urban breezes and mountain slope winds in the presence of basic-state wind

Jaemyeong Mango Seo<sup>1</sup> · Gantuya Ganbat<sup>1</sup> · Ji-Young Han<sup>2</sup> · Jong-Jin Baik<sup>1</sup>

Received: 8 April 2015 / Accepted: 4 November 2015 / Published online: 13 November 2015  
© Springer-Verlag Wien 2015

**Abstract** Many big cities around the world are located near mountains. In city-mountain regions, thermally and topographically forced local winds are produced and they affect the transport of pollutants emitted into the urban atmosphere. A better understanding of the dynamics of thermally and topographically forced local winds is necessary to improve the prediction of local winds and to cope with environmental problems. In this study, we theoretically examine the interactions of urban breezes with mountain slope winds in the presence of basic-state wind within the context of the response of a stably stratified atmosphere to prescribed thermal and mechanical forcing. The interactions between urban breezes and mountain slope winds are viewed through the linear superposition of individual analytical solutions for urban thermal forcing, mountain thermal forcing, and mountain mechanical forcing. A setting is considered in which a city is located downwind of a mountain. In the nighttime, in the mountain-side urban area, surface/near-surface horizontal flows induced by mountain cooling and mountain mechanical forcing cooperatively interact with urban breezes, resulting in strengthened winds. In the daytime, in the urban area, surface/near-surface horizontal flows induced by mountain heating are opposed to urban breezes, giving rise to weakened winds. It is shown that the degree of interactions between urban breezes and mountain slope winds is sensitive to mountain

height and basic-state wind speed. Particularly, a change in basic-state wind speed affects not only the strength of thermally and mechanically induced flows (internal gravity waves) but also their vertical wavelength and decaying rate. The examination of a case in a setting in which a city is located upwind of a mountain reveals that basic-state wind direction is an important factor that significantly affects the interactions of urban breezes with mountain slope winds.

## 1 Introduction

Many interesting thermally or mechanically driven local-wind phenomena are observed in the atmosphere, including urban breezes, land/sea breezes, mountain/valley winds, severe downslope storms, etc. Over the past few decades, these local-wind phenomena have been extensively studied and substantial progress in understanding the basic dynamics of each local-wind phenomenon has been made (see references in Simpson (1994), Lin (2007), and Markowski and Richardson (2010)). In many regions of the world, local-wind systems interact with each other. The degree of interactions between local-wind systems differs depending on location, time of day, etc. For example, daytime urban breezes interact with sea breezes in and around coastal/inland cities and the degree of the interactions differs depending on many factors, such as sea surface temperature, city size, urban heat island intensity, and time of day (e.g., Yoshikado 1992; Freitas et al. 2007; Ryu and Baik 2013). Understanding the dynamics of interactions between local-wind systems is one of the important issues in mesoscale dynamics and helps to cope with environmental problems with which big cities located near mountains or in complex terrain or adjacent to seas

✉ Jong-Jin Baik  
jjaik@snu.ac.kr

<sup>1</sup> School of Earth and Environmental Sciences, Seoul National University, Seoul 151-742, South Korea

<sup>2</sup> Korea Institute of Atmospheric Prediction Systems, Seoul 156-849, South Korea

are faced. Fernando (2010) reviewed the fluid dynamics of mesoscale urban airflows in complex terrain.

Thermally or mechanically driven winds/flows can be theoretically investigated from the viewpoint of the response of a stably stratified atmosphere to prescribed thermal or mechanical forcing. From this angle, extensive theoretical studies, particularly focusing on mountain waves or convectively forced flows, have been performed to better understand thermally or mechanically driven winds/flows (e.g., Queney 1948; Smith 1980; Lin 1987; Song and Chun 2005). The interactions between mountain waves and convectively forced flows with application to the dynamics of orographic rain are well described in a theoretical study of Smith and Lin (1982).

Recently, Ganbat et al. (2015) theoretically examined the interactions of urban breezes with mountain slope winds in the absence of basic-state wind. When there is no basic-state wind, mountains cannot mechanically induce mountain waves in a stably stratified atmosphere. Hence, mountain slope winds are produced only by mountain thermal forcing (mountain heating in the daytime and mountain cooling in the nighttime). In this study, we extend our previous study by including basic-state wind and mountain mechanical forcing and further examine the interactions of urban breezes with mountain slope winds. The sensitivities of the interactions to mountain mechanical forcing and basic-state wind speed are also investigated. In this study, mountain slope winds are produced by both mountain thermal forcing and mountain mechanical forcing. In Section 2, governing equations and solutions are provided. In Section 3, values of parameters for calculations are provided. In Section 4, calculation results are presented and discussed. Finally, conclusions are provided in Section 5.

## 2 Governing equations and analytical solutions

In this study, a two-dimensional, hydrostatic, nonrotating, Boussinesq airflow system in the presence of thermal forcing and topography is considered. Linearized equations in the presence of uniform basic-state horizontal wind can be expressed as follows (Lin 2007; Ganbat et al. 2015):

$$\frac{\partial u}{\partial t} + U \frac{\partial u}{\partial x} = - \frac{\partial \pi}{\partial x} - vu, \quad (1)$$

$$\frac{\partial \pi}{\partial z} = b, \quad (2)$$

$$\frac{\partial b}{\partial t} + U \frac{\partial b}{\partial x} + N^2 w = \frac{g}{c_p T_0} q - vb, \quad (3)$$

$$\frac{\partial u}{\partial x} + \frac{\partial w}{\partial z} = 0. \quad (4)$$

Here,  $u$  is the perturbation velocity in the  $x$ -direction,  $w$  is the perturbation velocity in the  $z$ -direction,  $\pi$  is the perturbation kinematic pressure, and  $b$  is the perturbation buoyancy.  $U$  is the basic-state wind speed in the  $x$ -direction,  $N$  is the buoyancy frequency (constant in this study),  $g$  is the gravitational acceleration,  $c_p$  is the specific heat of air at constant pressure,  $T_0$  is the reference temperature, and  $\nu$  is the coefficient of Rayleigh friction and Newtonian cooling.  $q$  in Eq. (3) represents thermal forcing (heating or cooling) and is specified as

$$q(x, z, t) = q_0 \frac{a_q^2}{(x - c_q)^2 + a_q^2} e^{-z/H} \operatorname{Re}\{e^{i\Omega t}\}. \quad (5)$$

Here,  $q_0$  is the magnitude of the thermal forcing,  $a_q$  is the half-width of the bell-shaped function,  $c_q$  is the horizontal location of the center of the thermal forcing, and  $H$  is the  $e$ -folding depth of the thermal forcing.  $\Omega$  is the angular frequency of the diurnal variation. A bell-shaped mountain is considered in this study, which is given by

$$h(x) = h_m \frac{a_h^2}{(x - c_h)^2 + a_h^2}, \quad (6)$$

where  $h_m$  is the maximum mountain height,  $a_h$  is the half-width of the bell-shaped mountain, and  $c_h$  is the horizontal location of the mountain center. A bell-shaped function is widely used in theoretical studies to represent thermal forcing and mountain shape (e.g., Queney 1948; Smith and Lin 1982; Baik 1992) because it imitates real heating/cooling and an isolated mountain well and the Fourier transform of the bell-shaped function is mathematically simple.

Equations (1)–(4) can be combined to yield a single equation for the perturbation vertical velocity.

$$\left( \frac{\partial}{\partial t} + U \frac{\partial}{\partial x} + \nu \right)^2 \frac{\partial^2 w}{\partial z^2} + N^2 \frac{\partial^2 w}{\partial x^2} = \frac{g}{c_p T_0} \frac{\partial^2 q}{\partial x^2}. \quad (7)$$

Equation (7) is Fourier-transformed in  $x$  ( $\rightarrow k$ ) and  $t$  ( $\rightarrow \omega$ ) to get

$$\frac{d^2 \hat{w}}{dz^2} + N^2 \lambda^2 \hat{w} = \frac{g}{c_p T_0} \lambda^2 \hat{q}, \quad (8)$$

where

$$\begin{aligned} \lambda &= \frac{k}{(\omega + U k) - i\nu}, \\ \hat{q}(k, z, \omega) &= q_0 a_q e^{-ic_q k} e^{-a_q k} e^{-z/H} \frac{\delta(\omega - \Omega) + \delta(\omega + \Omega)}{2}. \end{aligned}$$

Here,  $\delta$  is the delta function. The solution of Eq. (8) is obtained by imposing an upper radiation condition ( $U > 0$  in

this study so that  $B = 0$ ) and a lower boundary condition of  $\hat{w} = ikU\hat{h}$  at  $z = 0$ .

$$\hat{w}(k, z, \omega) = ikU\hat{h}e^{iN\lambda z} + C \frac{\lambda^2}{1 + N^2\lambda^2H^2} e^{-ic_0k} e^{-a_qk} \frac{\delta(\omega - \Omega) + \delta(\omega + \Omega)}{2} (e^{-z/H} - e^{iN\lambda z}), \quad (9)$$

where

$$\begin{aligned} \hat{h}(k, \omega) &= h_m a_h e^{-ic_h k} e^{-a_h k} \delta(\omega), \\ C &= \frac{g}{c_p T_0} q_0 a_q H^2. \end{aligned}$$

Time-invariant property of  $h(x)$  is represented by  $\delta(\omega)$  in wavenumber-frequency space. The first term on the right-hand side of Eq. (9) represents the perturbation vertical velocity in the wavenumber-frequency space induced by the mountain mechanical forcing. The second term on the right-hand side of Eq. (9) represents the perturbation vertical velocity in the wavenumber-frequency space induced by the thermal forcing. To obtain the solution for the perturbation vertical velocity in physical space, the inverse Fourier transform in  $k$  ( $\rightarrow x$ ) and  $\omega$  ( $\rightarrow t$ ) upon Eq. (9) is performed and then the real part is taken.

$$\begin{aligned} w(x, z, t) = &-Uh_m a_h \int_0^\infty k e^{-a_h k} e^{-\gamma_0 z} \sin[k(x - c_h) + m_0 z] dk \\ &+ \frac{C}{2} \int_0^\infty k^2 e^{-a_q k} \left\langle X_R \left\{ e^{-z/H} \cos[k(x - c_q) + \Omega t] - e^{-\gamma z} \cos[k(x - c_q) + mz + \Omega t] \right\} \right. \\ &- X_I \left\{ e^{-z/H} \sin[k(x - c_q) + \Omega t] - e^{-\gamma z} \sin[k(x - c_q) + mz + \Omega t] \right\} \\ &+ X_R' \left\{ e^{-z/H} \cos[k(x - c_q) - \Omega t] - e^{-\gamma' z} \cos[k(x - c_q) + m' z - \Omega t] \right\} \\ &\left. - X_I' \left\{ e^{-z/H} \sin[k(x - c_q) - \Omega t] - e^{-\gamma' z} \sin[k(x - c_q) + m' z - \Omega t] \right\} \right\rangle dk, \end{aligned} \quad (10)$$

where

$$\begin{aligned} X_R &= \frac{(\Omega + Uk)^2 + N^2 H^2 k^2 - \nu^2}{\left[ (\Omega + Uk)^2 + N^2 H^2 k^2 - \nu^2 \right]^2 + 4\nu^2(\Omega + Uk)^2}, \\ X_I &= \frac{2\nu(\Omega + Uk)}{\left[ (\Omega + Uk)^2 + N^2 H^2 k^2 - \nu^2 \right]^2 + 4\nu^2(\Omega + Uk)^2}, \\ X_R' &= \frac{(\Omega - Uk)^2 + N^2 H^2 k^2 - \nu^2}{\left[ (\Omega - Uk)^2 + N^2 H^2 k^2 - \nu^2 \right]^2 + 4\nu^2(\Omega - Uk)^2}, \\ X_I' &= \frac{-2\nu(\Omega - Uk)}{\left[ (\Omega - Uk)^2 + N^2 H^2 k^2 - \nu^2 \right]^2 + 4\nu^2(\Omega - Uk)^2}, \\ \gamma_0 &= \frac{Nk\nu}{U^2 k^2 + \nu^2}, \quad m_0 = \frac{NUk^2}{U^2 k^2 + \nu^2}, \\ \gamma &= \frac{Nk\nu}{(\Omega + Uk)^2 + \nu^2}, \quad m = \frac{Nk(\Omega + Uk)}{(\Omega + Uk)^2 + \nu^2}, \\ \gamma' &= \frac{Nk\nu}{(\Omega - Uk)^2 + \nu^2}, \quad m' = \frac{-Nk(\Omega - Uk)}{(\Omega - Uk)^2 + \nu^2}. \end{aligned}$$

Using the forward Euler scheme, the numerical integration with respect to  $k$  in Eq. (10) is made. We use  $k_n = 2n\pi/10^5 \text{ m}^{-1}$  ( $n = 1, 2, \dots, 10,000$ ) which gives  $L_x = 10\text{--}10^5 \text{ m}$  ( $L_x$ , wavelength in the  $x$ -direction). The choice of the domain size does not matter if  $L_x$  corresponding to the smallest  $k$  ( $k_1$ ) covers the entire domain and  $L_x$  corresponding to the largest  $k$  ( $k_{10,000}$ ) is smaller than the  $x$ -directional resolution. In this study,  $\Delta x = 100 \text{ m}$  is used. Using Eq. (10) and the Fourier-transformed equations of

Eqs. (1)–(4), the solutions for the perturbation horizontal velocity, perturbation kinematic pressure, and perturbation buoyancy can be obtained. Note that in the absence of the mountain mechanical forcing, the solution  $w$  becomes identical to that of Ganbat et al. (2015).

### 3 Parameters

The solution that represents the linear interactions of urban breezes with mountain slope winds is obtained by the linear superposition of solutions that correspond to urban thermal forcing, mountain thermal forcing, and mountain mechanical forcing. The thermal forcing that induces urban breezes and the thermal forcing that induces mountain slope winds are supposed to have steady components ( $\Omega = 0 \text{ s}^{-1}$ ) and diurnally varying components ( $\Omega = 2\pi/24 \text{ h}^{-1}$ ) (Ganbat et al. 2015). Mountain mechanical forcing has a steady component only. The solution for the perturbation vertical velocity is the sum of solutions corresponding to each forcing, which is given by

$$\begin{aligned} w(x, z, t) = &w_{us}(x, z) + w_{ud}(x, z, t - \tau_u) \\ &+ w_{ms}(x, z) + w_{md}(x, z, t - \tau_m) + w_h(x, z). \end{aligned} \quad (11)$$

Here,  $w_{us}$ ,  $w_{ud}$ ,  $w_{ms}$ , and  $w_{md}$  are the perturbation vertical velocities corresponding to the steady urban thermal

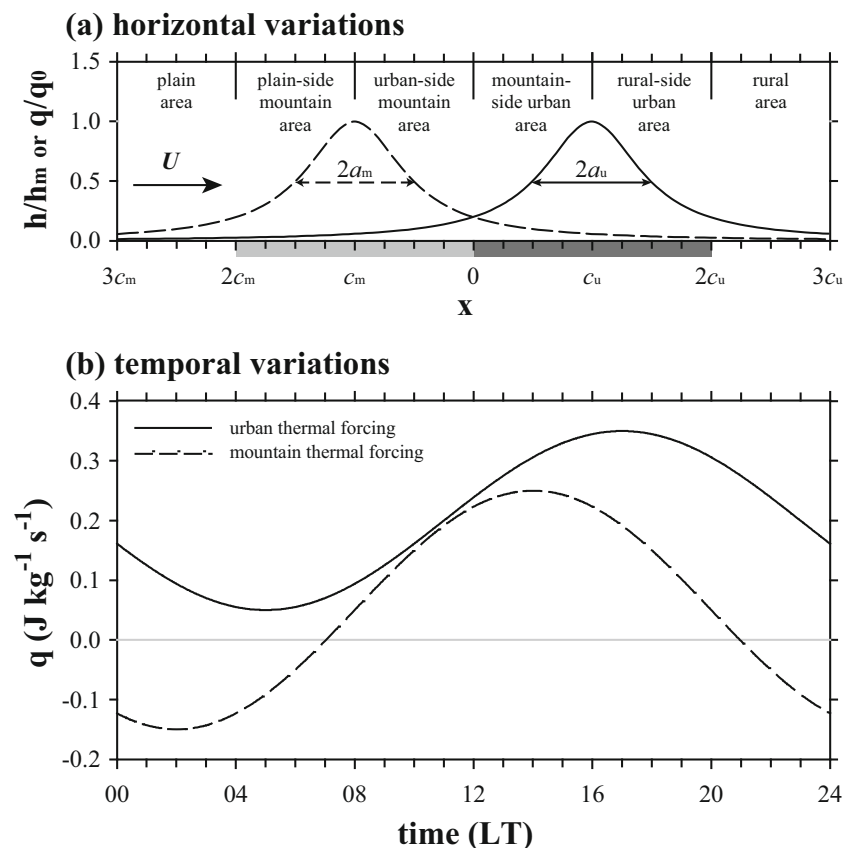
forcing, diurnally varying urban thermal forcing, steady mountain thermal forcing, and diurnally varying mountain thermal forcing, respectively. The magnitudes of steady urban thermal forcing, diurnally varying urban thermal forcing, steady mountain thermal forcing, and diurnally varying mountain thermal forcing are denoted by  $q_{us}$ ,  $q_{ud}$ ,  $q_{ms}$ , and  $q_{md}$ , respectively.  $\tau_u$  is the time of maximum urban thermal forcing, and  $\tau_m$  is the time of maximum mountain thermal forcing.  $w_h$  is the perturbation vertical velocity corresponding to steady mountain mechanical forcing.

Consider a setting in which a city is located downwind of a mountain. The center of the city (mountain) is located at  $x = 10$  km ( $x = -10$  km). Following Ganbat et al. (2015), the following parameter values are used in the calculations:  $q_{us} = 0.20 \text{ J kg}^{-1} \text{ s}^{-1}$ ,  $q_{ud} = 0.15 \text{ J kg}^{-1} \text{ s}^{-1}$ ,  $q_{ms} = 0.05 \text{ J kg}^{-1} \text{ s}^{-1}$ ,  $q_{md} = 0.20 \text{ J kg}^{-1} \text{ s}^{-1}$ ,  $c_u = 10 \text{ km}$ ,  $c_m = -10 \text{ km}$ ,  $\tau_u = 1700 \text{ LT}$ ,  $\tau_m = 1400 \text{ LT}$ ,  $a_u = a_m = 5 \text{ km}$ ,  $H_u = 750 \text{ m}$  (urban  $H$ ),  $H_m = 500 \text{ m}$  (mountain  $H$ ),  $N = 0.01 \text{ s}^{-1}$ ,  $T_0 = 283 \text{ K}$ , and  $\nu = 1/7200 \text{ s}^{-1}$ . Even though the time variation of buoyancy frequency affects thermally or mechanically induced flows,  $N$  is treated as a constant because of mathematical difficulty in handling time-dependent buoyancy frequency. For simplicity, a region of  $x = 0$  to  $20$  km ( $x = -20$  to  $0$  km) is called the

urban (mountain) area. In a control case, the basic-state wind speed is specified as  $2 \text{ m s}^{-1}$ , and the maximum mountain height is specified as  $100 \text{ m}$ . Sensitivities to mountain height and basic-state wind speed are examined.

The horizontal variations of urban thermal forcing and mountain thermal and mechanical forcings normalized by the maximum of each forcing are plotted in Fig. 1a. Figure 1a also shows the names of the areas which are used in this study (mountain-side urban area, rural-side urban area, urban-side mountain area, and plain-side mountain area). The dark gray (gray) box on the  $x$ -axis indicates the urban (mountain) area. The temporal variations of urban thermal forcing and mountain thermal forcing at the center of each thermal forcing and  $z = 0 \text{ km}$  are shown in Fig. 1b, which is from Ganbat et al. (2015). Note that urban (mountain) thermal forcing is the sum of steady urban (mountain) thermal forcing and the diurnally varying urban (mountain) thermal forcing. Urban thermal forcing is positive at all times (urban heating), and mountain thermal forcing is positive from 0700 to 2100 LT (mountain heating) and negative from 2100 to 0700 LT (mountain cooling) (Fig. 1b). In the following sections, the perturbation vertical velocity, perturbation horizontal velocity, perturbation velocity vector, perturbation buoyancy, and perturbation

**Fig. 1** **a** Horizontal variations of urban thermal forcing (solid line) and mountain thermal and mechanical forcings (dashed line) normalized by the maximum of each forcing. The dark gray (gray) box on the  $x$ -axis indicates the urban (mountain) area. The names of the areas used in this study are given. **b** Temporal variations of urban thermal forcing at  $x = c_u$  and  $z = 0 \text{ km}$  (solid line) and mountain thermal forcing at  $x = c_m$  and  $z = 0 \text{ km}$  (dashed line). **(b)** is from Ganbat et al. (2015)



kinematic pressure are called as the vertical velocity, horizontal velocity, velocity vector, buoyancy, and kinematic pressure for brevity, respectively.

## 4 Results and discussion

### 4.1 Cases with each forcing only

To facilitate an investigation of the interactions of urban breezes with mountain slope winds, the results of cases with each forcing only are first presented. Figure 2 shows the vertical velocity, velocity vector, buoyancy, and kinematic pressure fields at 0200 and 1700 LT in the cases with urban thermal forcing only, mountain thermal forcing only, and mountain mechanical forcing only. In all three cases, the basic-state wind speed is specified as  $2 \text{ m s}^{-1}$ . In the case with mountain mechanical forcing only, the maximum mountain height is specified as 100 m. In all three cases, updraft and downdraft bands in the vertical direction are

evident, especially in the case with mountain mechanical forcing only. These updraft and downdraft bands are internal gravity waves forced by thermal or mechanical forcing in a stably stratified atmosphere (Baik and Chun 1997). Wave amplitudes decrease with height because of the exponential decay of urban or mountain thermal forcing (thermal forcing is zero in the case with mountain mechanical forcing only) and the Rayleigh friction and Newtonian cooling. Phase lines are tilted upwind, implying upward propagation of wave energy (Chun and Baik 1998).

In the case with urban heating only (Fig. 2a, b), the buoyancy and kinematic pressure gradient in the urban area are larger at 1700 LT than at 0200 LT because of stronger urban heating at 1700 LT. This leads to stronger circulation at 1700 LT than at 0200 LT. At 1700 LT, relatively strong upward motion is observed downwind of the urban heating center ( $x = 10 \text{ km}$ ), while weak downward motion is observed upwind of the urban heating center. This result is consistent with that of Baik (1992). In the urban area, positive surface/near-surface (perturbation) horizontal flows are observed and

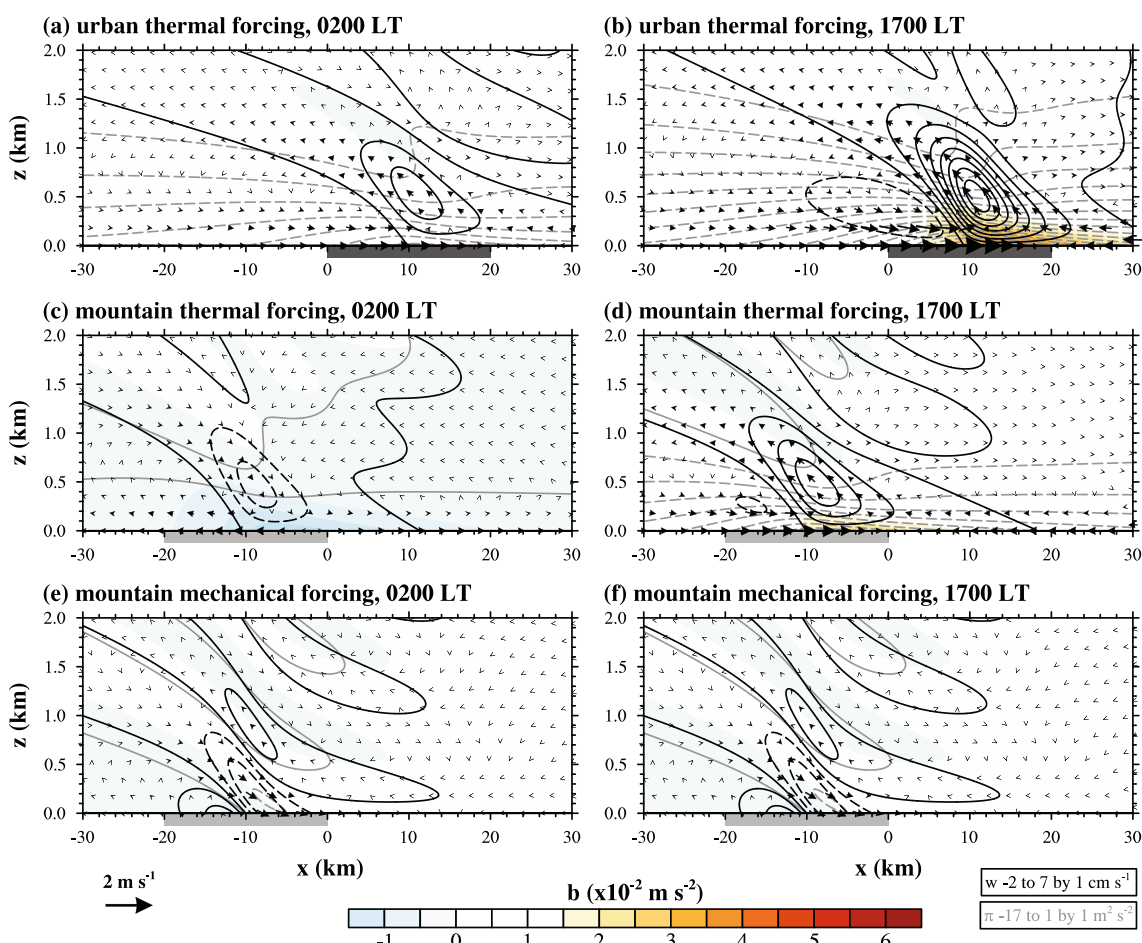


**Fig. 2** Vertical velocity (black lines), velocity vector, buoyancy (shaded), and kinematic pressure (gray lines) fields at 0200 LT (left) and 1700 LT (right) in the cases with **a, b** urban thermal forcing only, **c, d** mountain thermal forcing only, and **e, f** mountain mechanical forcing only

only. The basic-state wind speed is specified as  $2 \text{ m s}^{-1}$ . In the case with mountain mechanical forcing only, the maximum mountain height is specified as 100 m. The dark gray (gray) box on the  $x$ -axis (also, in Figs. 3, 4, 5, and 6) indicates the urban (mountain) area

they diverge and then converge as going downwind. The location of maximum surface convergence, which is  $x = 14.2$  km at 1700 LT, is situated downwind of the urban heating center. In  $x = -10$  to 0 km, there are positive horizontal flows at low levels. These features are also observed at 0200 LT, although urban-heating induced flows are weaker. In the case with mountain thermal forcing only (Fig. 2c, d), there is mountain cooling at 0200 LT and mountain heating at 1700 LT (Fig. 1b). In  $x = -10$  to 0 km, downward motion at 0200 LT and upward motion at 1700 LT exist. In the mountain area, there exists negative surface/near-surface horizontal flows except near  $x = 0$  km at 0200 LT and positive surface/near-surface horizontal flows at 1700 LT. In  $x = 0$  to 10 km, positive horizontal flows at 0200 LT and negative horizontal flows at 1700 LT are observed at low levels. In the case with mountain mechanical forcing only (Fig. 2e, f), the perturbation field at 0200 LT is identical to that at 1700 LT because mountain mechanical forcing is steady. At low levels, downslope winds (downward motion with positive horizontal flows) are produced in  $x = -10$  to 0 km. In  $x = 0$  to 10 km, positive surface/near-surface horizontal flows are produced, but their intensity is very weak.

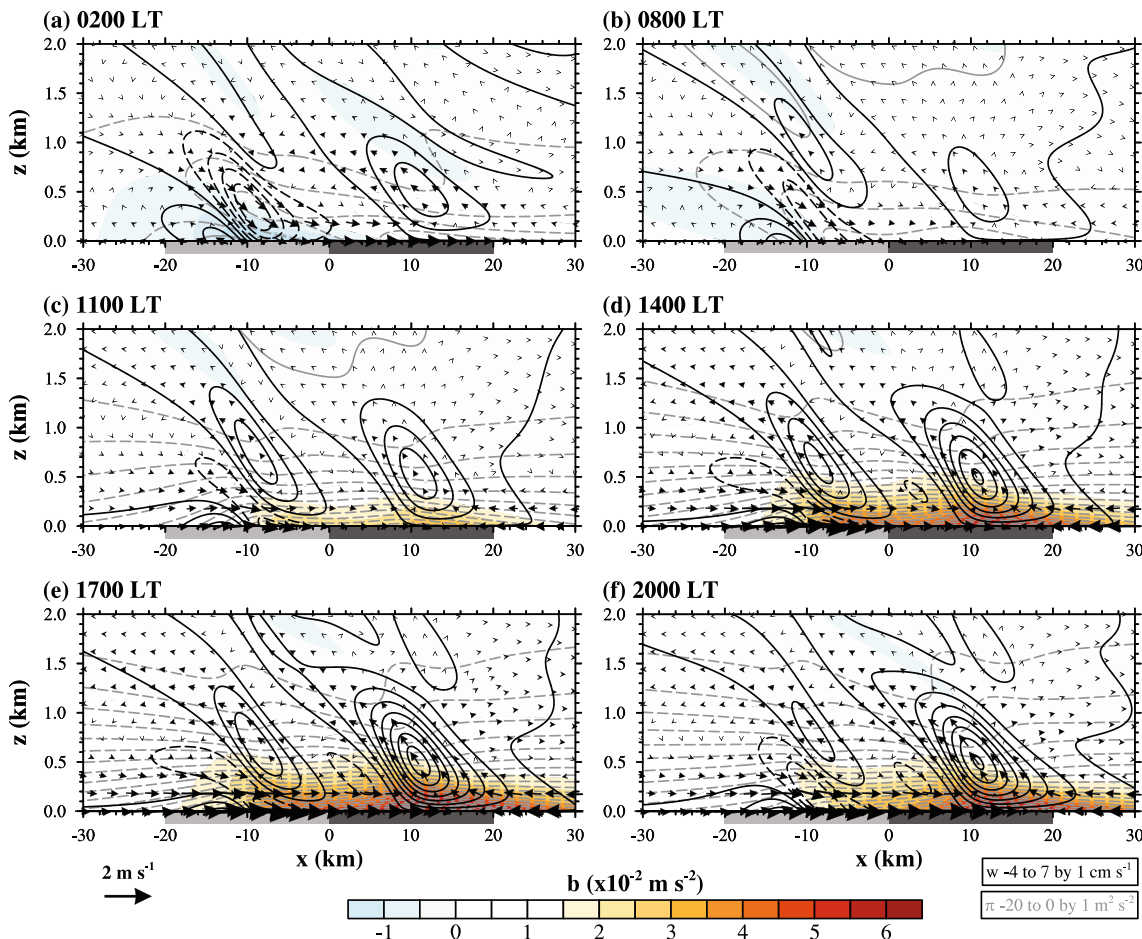


**Fig. 3** Vertical velocity (black lines), velocity vector, buoyancy (shaded), and kinematic pressure (gray lines) fields at **a** 0200, **b** 0800, **c** 1100, **d** 1400, **e** 1700, and **f** 2000 LT in the control case

## 4.2 Control case

The control case is equal to a case that linearly combines the three cases with each forcing only (Fig. 2). Figure 3 shows the vertical velocity, velocity vector, buoyancy, and kinematic pressure fields at 0200, 0800, 1100, 1400, 1700, and 2000 LT in the control case ( $U = 2 \text{ m s}^{-1}$  and  $h_m = 100 \text{ m}$ ). Flow patterns in the presence of basic-state wind (Fig. 3) are quite different from those in the absence of basic-state wind (Ganbat et al. 2015). Unlike in Ganbat et al. (2015), updraft and down-draft bands in the vertical direction with phase lines tilted upwind are produced in the control case.

At 0200 LT (Fig. 3a), urban heating produces upward motion in the rural-side urban area ( $x = 10$  to 20 km). Mountain cooling produces downward motion on the urban-side mountain slope ( $x = -10$  to 0 km), and mountain mechanical forcing produces downslope winds on the urban-side mountain slope. On the urban-side mountain slope, downward motion induced by mountain cooling is cooperatively combined with downslope winds induced by mountain mechanical forcing, resulting in strengthened downward motion. On the other hand, on the urban-side mountain slope, negative surface/

near-surface horizontal flows induced by mountain cooling are opposed to the horizontal component of downslope winds induced by mountain mechanical forcing, resulting in weakened positive surface/near-surface horizontal flows. In the mountain-side urban area ( $x = 0$  to 10 km), positive surface/near-surface horizontal flows induced by mountain cooling and very weak positive surface/near-surface horizontal flows induced by mountain mechanical forcing are cooperatively combined with urban breezes, giving rise to strengthened winds. At 0800 LT (Fig. 3b), mountain heating is weak (Fig. 1b), so mountain mechanical forcing plays an important role in producing mountain slope winds. Upward motion in the rural-side urban area is weaker at 0800 LT than at 0200 LT. Urban heating at 0800 LT is the same as that at 0200 LT, and mountain mechanical forcing is steady. Hence, mountain heating is responsible for the weaker upward motion at 0800 LT in the rural-side urban area, which is associated with weaker surface/near-surface convergence. At 1100 LT (Fig. 3c), both urban heating and mountain heating increase (Fig. 1b). Upward motion in the rural-side urban area is further intensified.

At 1400 LT (Fig. 3d), mountain heating is the strongest (Fig. 1b), producing strong upward motion on the urban-side mountain area ( $x = -10$  to 0 km). On the urban-side mountain slope, downslope winds induced by mountain mechanical forcing and upward motion induced by mountain heating act oppositely to give rise to weakened downward motion. Because urban heating is also strong at 1400 LT, upward motion stronger at 1100 LT develops in the rural-side urban area. Because of the influences of downslope winds induced by mountain mechanical forcing and urban breezes induced by urban heating, winds on the urban-side mountain slope are directed toward the urban center. At 1700 LT (Fig. 3e), urban heating is the strongest (Fig. 1b) and the buoyancy in the urban area is positive and large, producing well-developed urban circulation with strong upward motion. The buoyancy in the urban area is larger in the control case than in the case with urban heating only (Fig. 2b). This is a result of the influence of mountain heating and the interactions of urban breezes with mountain slope winds. Because of strengthened urban breezes, winds toward the urban center on the urban-side mountain slope become strong. At 2000 LT (Fig. 3f), mountain heating is weak (Fig. 1b) and mountain mechanical forcing is mainly responsible for mountain slope winds.

As should be expected, Fig. 3 shows that the interactions of urban breezes with mountain slope winds are stronger in the area between the mountain center and the urban center than in other areas, simply because of larger superposition of urban heating, mountain thermal forcing, and mountain mechanical forcing. In the mountain-side urban area, in the nighttime and daytime, surface/near-surface winds are directed toward the urban center due to urban heating, but their intensity changes with time, depending on diurnally varying interactions

between urban breezes and mountain slope winds. In the urban-side mountain area, mountain cooling in the nighttime and mountain heating in the daytime play a crucial role in diurnally varying interactions between urban breezes and mountain slope winds.

#### 4.3 Sensitivities to mountain height and basic-state wind speed

The degree of interactions between urban breezes and mountain slope winds can vary depending on the magnitudes of basic-state wind speed and stability as well as on the intensities of urban thermal forcing, mountain thermal forcing, and mountain mechanical forcing. In this subsection, we examine the sensitivities of the interactions of urban breezes with mountain slope winds to mountain height and basic-state wind speed. The maximum mountain height ( $h_m$ ) is a parameter that controls the intensity of mountain mechanical forcing.

Figure 4 shows the vertical velocity, velocity vector, buoyancy, and kinematic pressure fields at 0200 and 1700 LT in the cases with  $h_m = 50$  and 200 m. These two cases are the same as the control case ( $h_m = 100$  m) except for the maximum mountain height. 0200 LT and 1700 LT are selected because representative nighttime and daytime flow features are well captured at these times. Equation (10) indicates that the vertical velocity induced by mountain mechanical forcing is proportional to maximum mountain height. Therefore, stronger (weaker) mountain mechanical forcing corresponding to a larger (smaller) maximum mountain height produces stronger (weaker) mountain waves in the mountain area, as seen in Figs. 3a, e and 4a. At 0200 LT, as mountain height increases, downward motion on the urban-side mountain slope, which is produced by downward motion induced by mountain cooling being combined with downslope winds induced by mountain mechanical forcing, is strengthened (Figs. 3a and 4a, c). On the urban-side mountain slope, downslope winds whose horizontal component is weakened due to negative horizontal flows induced by mountain cooling intensify with increasing mountain height. Stronger downslope winds toward the city center for stronger mountain mechanical forcing are cooperatively combined with urban breezes in the mountain-side urban area. This leads to strengthened winds in the mountain-side urban area with increasing mountain height, as seen in Figs. 3a and 4a, c. The intensity of upward motion in the rural-side urban area changes little with mountain height. At 1700 LT, winds on the urban-side mountain slope intensify, and accordingly, winds in the mountain-side urban area also intensify as mountain height increases (Figs. 3e and 4b, d).

Sensitivity to basic-state wind speed is shown in Fig. 5, depicting the vertical velocity, velocity vector, buoyancy, and kinematic pressure fields at 0200 and 1700 LT in the cases

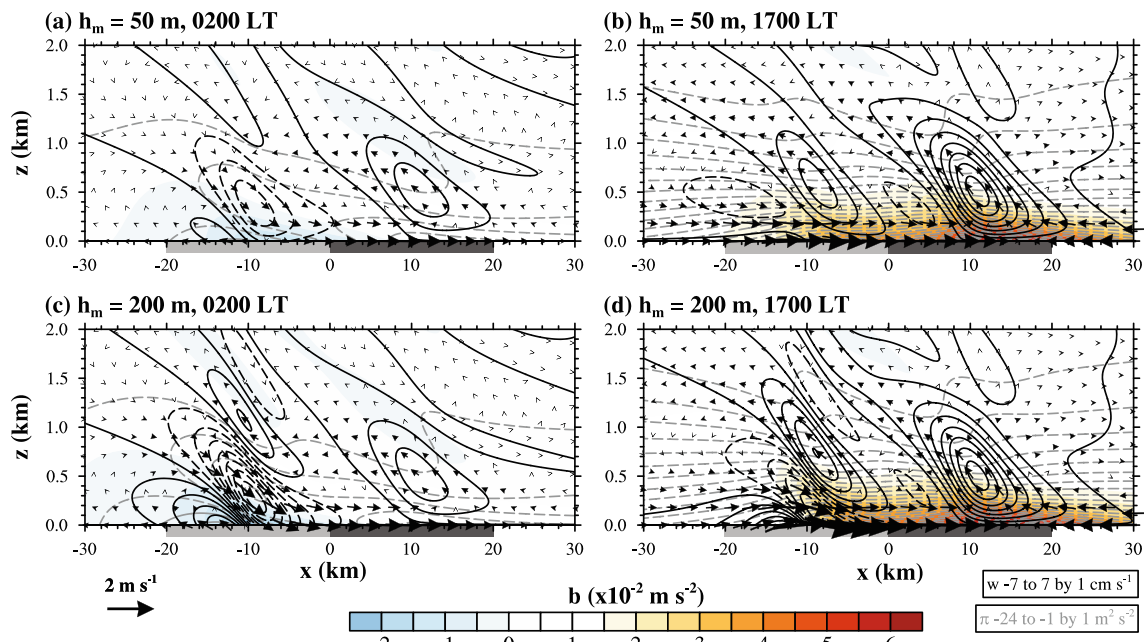


**Fig. 4** Vertical velocity (black lines), velocity vector, buoyancy (shaded), and kinematic pressure (gray lines) fields at 0200 LT (left) and 1700 LT (right) in the cases with **a, b**  $h_m = 50$  m and **c, d**  $h_m = 200$  m. The basic-state wind speed is specified as  $2 \text{ m s}^{-1}$

with  $U = 1$  and  $4 \text{ m s}^{-1}$ . These two cases are the same as the control case ( $U = 2 \text{ m s}^{-1}$ ) except for basic-state wind speed. A change in basic-state wind speed affects not only the strength of thermally and mechanically induced flows (internal gravity waves) but also their vertical wavelength and decaying rate (Eq. 10). As basic-state wind speed increases, thermally and mechanically induced flows are extended deeper in the vertical direction, mountain waves induced by mountain

mechanical forcing intensify, and the vertical wavelength of updraft and downdraft bands increases (Figs. 3a, e and 5). As basic-state wind speed increases, at 0200 LT, surface/near-surface horizontal flows directed toward the city center in the area between the mountain center and the urban center weaken. In the case with  $U = 4 \text{ m s}^{-1}$ , positive surface/near-surface horizontal flows are present outside of the urban area as well as in the urban area (Fig. 5c). At 1700 LT, winds on the

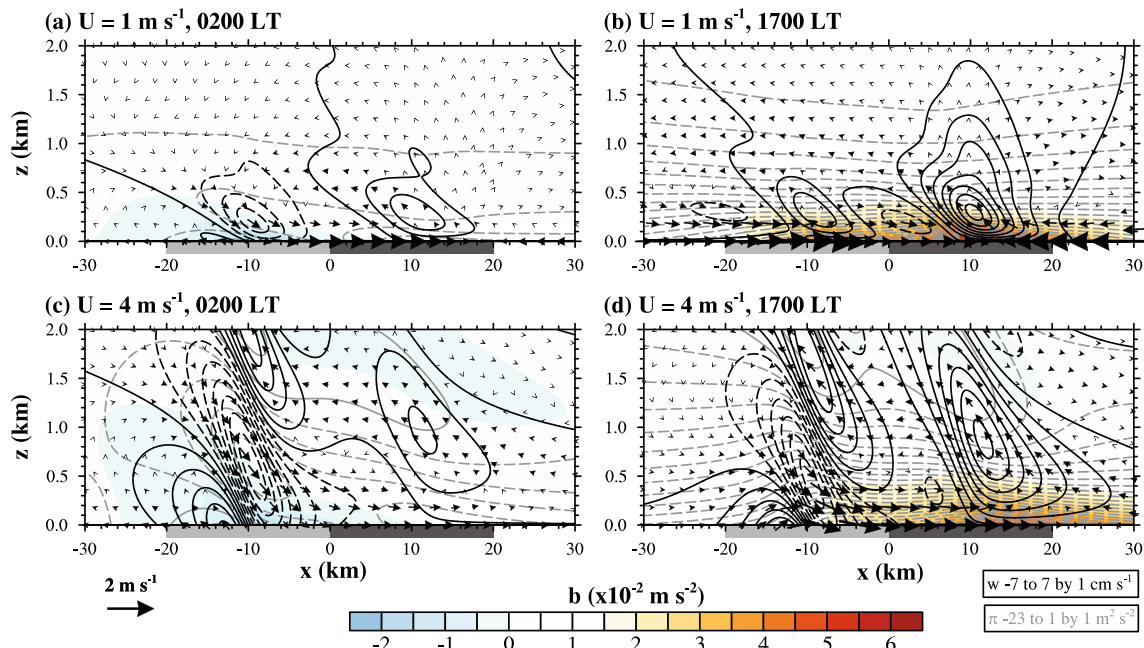


**Fig. 5** Vertical velocity (black lines), velocity vector, buoyancy (shaded), and kinematic pressure (gray lines) fields at 0200 LT (left) and 1700 LT (right) in the cases with **a, b**  $U = 1 \text{ m s}^{-1}$  and **c, d**  $U = 4 \text{ m s}^{-1}$ . The maximum mountain height is specified as 100 m

urban-side mountain slope become strong and surface/near-surface horizontal flows in the mountain-side urban area strengthen as basic-state wind speed increases (Figs. 3e and 5b, d). The location of zero surface horizontal flows is shifted farther downwind with increasing basic-state wind speed (Figs. 3e and 5b, d). Because  $w_h$  is explicitly proportional to  $U$ , but  $w_{us}$ ,  $w_{ud}$ ,  $w_{ms}$ , or  $w_{md}$  is approximately proportional to  $U^2$  (Eq. 10), mountain mechanical forcing becomes more important with increasing basic-state wind speed, as clearly seen in Fig. 5.

Thus far, we have investigated the interactions of urban breezes with mountain slope winds in the cases in which a city is located downwind of a mountain. Here, we examine interactions between urban breezes and mountain slope winds in a setting in which a city is located upwind of a mountain. In a case considered, the urban area is situated upwind of the mountain area with the urban and mountain centers being located at  $x = -10$  km and  $x = 10$  km, respectively, and other specified parameter values are the same as those in the control case. This case is equivalent to the control case, but with basic-state wind blowing in the opposite direction ( $U < 0$ ). At 0200 LT (Fig. 6a), strengthened upward motion by mountain cooling and mountain mechanical forcing on the urban-side mountain slope ( $x = 0$  to 10 km) is connected with upward

motion induced by urban heating on the mountain-side urban area ( $x = -10$  to 0 km), forming a broad region of upward motion between the urban center and the mountain center. Surface/near-surface horizontal flows in the mountain-side urban area are weaker than those in the control case (Figs. 3a and 6a). At 1700 LT (Fig. 6b), the connected upward motion still exists, but its intensity on the urban-side mountain slope is weaker than that at 0200 LT. This weaker intensity is because on the urban-side mountain slope, upward motion induced by mountain mechanical forcing is combined with downward motion induced by mountain heating. On the urban-side mountain slope, surface/near-surface horizontal flows are very weak because negative surface/near-surface horizontal flows induced by urban heating are almost cancelled by positive surface/near-surface horizontal flows induced by mountain heating. Figures 3 and 6 indicate that basic-state wind direction is one of the important factors that significantly affect interactions between urban breezes and mountain slope winds.

## 5 Conclusions

In this theoretical study, we extended our previous study (Ganbat et al. 2015) by including basic-state wind and mountain mechanical forcing to further examine the interactions of urban breezes with mountain slope winds. We showed how interactions between urban breezes and mountain slope winds vary diurnally and differ location by location. Further, we showed that the degree of interactions between urban breezes and mountain slope winds is sensitive to mountain height and basic-state wind speed and that basic-state wind direction is an important factor that significantly affects these interactions. This study demonstrates the virtue of the linear mesoscale dynamics of local winds in city-mountain areas.

In this theoretical study, the buoyancy frequency, i.e., the basic-state stability, is assumed to be constant and the two-dimensional airflow system is adapted. Noticing the importance of basic-state stability in thermally and mechanically forced winds/flows and the common geometries of cities, time-varying basic-state stability and extension to three dimensions need to be taken into account in future research. In this theoretical study, the Coriolis force is neglected. The effects of the Coriolis force on interactions between urban breezes and mountain slope winds deserve an investigation. Although the linear dynamics can explain many aspects of interactions between urban breezes and mountain slope winds, there may be other aspects of the interactions that cannot be explained with the linear dynamics or in which nonlinear dynamics is important. A challenging research topic would be to examine nonlinear interactions between urban breezes and mountain slope winds using nonlinear theories or simple nonlinear dynamical models.

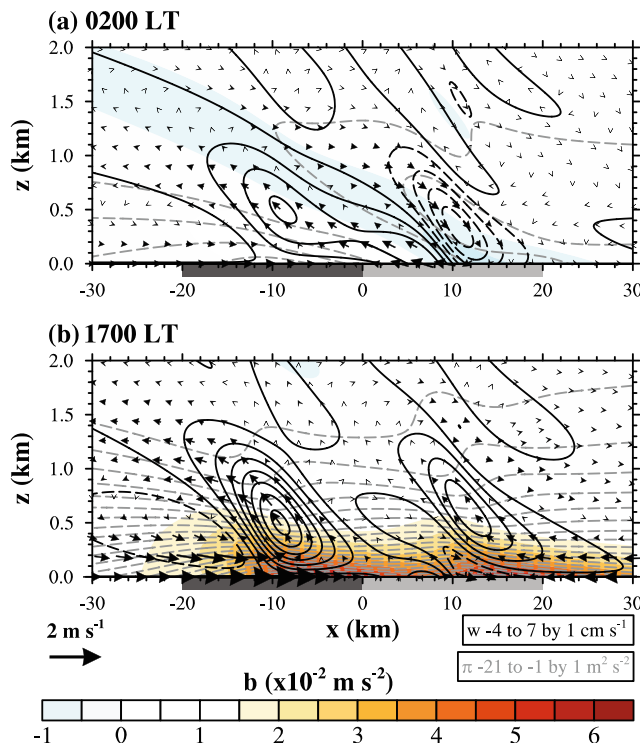


**Fig. 6** Vertical velocity (black lines), velocity vector, buoyancy (shaded), and kinematic pressure (gray lines) fields at **a** 0200 LT and **b** 1700 LT in the case in which a city is located upwind of a mountain. The maximum mountain height and basic-state wind speed are specified as 100 m and  $2 \text{ m s}^{-1}$ , respectively

**Acknowledgments** The authors are grateful to two anonymous reviewers for providing valuable comments on this work. The first, second, and fourth authors were supported by the National Research Foundation of Korea (NRF) grant funded by the Korea Ministry of Science, ICT and Future Planning (MSIP) (No. 2011-0017014) and also by the Korea Meteorological Administration Research and Development Program under grant KMIPA 2015-5100. The third author was supported by the R&D project on the development of Korea's global numerical weather prediction systems of Korea Institute of Atmospheric Prediction Systems (KIAPS) funded by the Korea Meteorological Administration (KMA).

## References

- Baik JJ (1992) Response of a stably stratified atmosphere to low-level heating—an application to the heat island problem. *J Appl Meteorol* 31:291–303
- Baik JJ, Chun HY (1997) A dynamical model for urban heat islands. *Bound-Layer Meteorol* 83:463–477
- Chun HY, Baik JJ (1998) Momentum flux by thermally induced internal gravity waves and its approximation for large-scale models. *J Atmos Sci* 55:3299–3310
- Fernando HJS (2010) Fluid dynamics of urban atmospheres in complex terrain. *Annu Rev Fluid Mech* 42:365–389
- Freitas ED, Rozoff CM, Cotton WR, Silva Dias PL (2007) Interactions of an urban heat island and sea-breeze circulations during winter over the metropolitan area of São Paulo, Brazil. *Bound-Layer Meteorol* 122:43–65
- Ganbat G, Seo JM, Han JY, Baik JJ (2015) A theoretical study of the interactions of urban breeze circulation with mountain slope winds. *Theor Appl Climatol* 121:545–555
- Lin YL (1987) Two-dimensional response of a stably stratified shear flow to diabatic heating. *J Atmos Sci* 44:1375–1393
- Lin YL (2007) Mesoscale dynamics. Cambridge University Press, Cambridge
- Markowski P, Richardson Y (2010) Mesoscale meteorology in midlatitudes. Wiley-Blackwell, Chichester
- Queney P (1948) The problem of airflow over mountains: a summary of theoretical studies. *Bull Am Meteorol Soc* 29:16–26
- Ryu YH, Baik JJ (2013) Daytime local circulations and their interactions in the Seoul metropolitan area. *J Appl Meteorol Climatol* 52:784–801
- Simpson JE (1994) Sea breeze and local wind. Cambridge University Press, Cambridge
- Smith RB (1980) Linear theory of stratified hydrostatic flow past an isolated mountain. *Tellus* 32:348–364
- Smith RB, Lin YL (1982) The addition of heat to a stratified airstream with application to the dynamics of orographic rain. *Q J R Meteorol Soc* 108:353–378
- Song IS, Chun HY (2005) Momentum flux spectrum of convectively forced internal gravity waves and its application to gravity wave drag parameterization. Part I: Theory *J Atmos Sci* 62:107–124
- Yoshikado H (1992) Numerical study of the daytime urban effect and its interaction with the sea breeze. *J Appl Meteorol* 31:1146–1164